Received 7 January 2021; revised 14 February 2021; accepted 22 February 2021. Date of publication 8 March 2021; date of current version 19 March 2021.

Digital Object Identifier 10.1109/OJCOMS.2021.3064504

An Error Rate Comparison of Power Domain Non-Orthogonal Multiple Access and Sparse Code Multiple Access

QU LUO [1] (Graduate Student Member, IEEE), PENGYU GAO[1], ZILONG LIU [2] (Senior Member, IEEE), LIXIA XIAO[3] (Member, IEEE), ZEINA MHEICH[1], PEI XIAO [1] (Senior Member, IEEE), AND AMINE MAAREF [4] (Senior Member, IEEE)

[1]5GIC & 6GIC, Institute for Communication Systems (ICS), University of Surrey, Guildford, GU2 7XH, U.K.

[2]School of Computer Science and Electronic Engineering, University of Essex, Colchester CO4 3SQ, U.K.

[3]Wuhan National Laboratory for Optoelectronics, Huazhong University of Science and Technology, Wuhan 430074, China

[4]Canada Research Center, Huawei Technologies Company Ltd., Ottawa, ON K2K 3J1, Canada

CORRESPONDING AUTHOR: P. XIAO (e-mail: p.xiao@surrey.ac.uk)

This work was supported by the U.K. Engineering and Physical Sciences Research Council under Grant EP/P03456X/1 and Grant EP/P008402/2.

ABSTRACT Non-orthogonal Multiple Access (NOMA) has been envisioned as one of the key enabling techniques to fulfill the requirements of future wireless networks. The primary benefit of NOMA is higher spectrum efficiency compared to Orthogonal Multiple Access (OMA). This paper presents an error rate comparison of two distinct NOMA schemes, i.e., power domain NOMA (PD-NOMA) and Sparse Code Multiple Access (SCMA). In a typical PD-NOMA system, successive interference cancellation (SIC) is utilized at the receiver, which however may lead to error propagation. In comparison, message passing decoding is employed in SCMA. To attain the best error rate performance of PD-NOMA, we optimize the power allocation with the aid of pairwise error probability and then carry out the decoding using generalized sphere decoder (GSD). Our extensive simulation results show that SCMA system with "5×10" setting (i.e., ten users communicate over five subcarriers, each active over two subcarriers) achieves better uncoded BER and coded BER performance than both typical "1×2" and "2×4" PD-NOMA systems in uplink Rayleigh fading channel. Finally, the impacts of channel estimation error on SCMA , SIC and GSD based PD-NOMA and the complexity of multiuser detection schemes are also discussed.

INDEX TERMS Non-orthogonal multiple access (NOMA), power domain NOMA (PD-NOMA), successive interference cancellation (SIC), generalized sphere decoder (GSD), sparse code multiple access (SCMA), bit error rate (BER).

I. INTRODUCTION

THE FIFTH-GENERATION (5G) networks and beyond are experiencing a paradigm shift from human-centric data services to machine-centric ones [1]. A major challenge here is how to support explosive growth of communication devices for massive connectivity. Non-Orthogonal Multiple Access (NOMA) schemes is regarded as an enabling technique which has received tremendous research attention from both academia and industry [2]–[5].

The key idea of NOMA is to allocate the invaluable system resources in a non-orthogonal fashion for overloaded multiuser communications. To date, numerous NOMA schemes have been proposed, which can be basically classified into two main categories, namely power-domain NOMA (PD-NOMA) [6]–[10] and code-domain NOMA [11]–[15]. PD-NOMA aims to multiplex two or more users sharing the same time and frequency resources by allocating them with different levels of power. By contrast, in code-domain NOMA, multiple users are mainly separated through non-orthogonal codebooks/sequences. The first scheme of code domain NOMA is referred as low density signature (LDS) [11]. This technique is motivated

by multi-carrier code division multiple access (MC-CDMA) by introducing spreading matrix. Later, in 2013, sparse code multiple access (SCMA) is proposed by Nikopour and Baligh [14]. Unlike LDS, SCMA encoder directly map the binary data to multidimensional complex domain codewords which are selected from pre-designed codebook.

Both PD-NOMA and SCMA systems are distinctive from each other with some unique features. In a PD-NOMA system, multiple users are first transmitted using superposition coding (SC) and then decoded by successive interference cancellation (SIC). On the other hand, SCMA, as a generalization of low-density signature CDMA (LDS-CDMA), enjoys the constellation shaping gain which stems from properly designed sparse codebooks. In SCMA, the bits streams are directly mapped to multidimensional complex codewords selected from a predefined codebook [14], [15]. Unlike SIC based multiuser detection (MUD), SCMA carries out the decoding with the aid of message passing algorithm (MPA) by exploiting the sparse structure of SCMA codewords. This allows SCMA to achieve a near-optimal bit error rate (BER) performance as well as a reduced complexity (compared that of the maximum-likelihood receiver).

A. LITERATURE

For the performance of PD-NOMA, the current studies mainly target at the sum-rate, outage probability and BER performance. In [16], [17], BER performance of downlink NOMA system with imperfect SIC over Nakagami-m fading channels has been studied thoroughly. Specifically, the closed-form expressions for the union bound on the BERs were derived in [16] while considering imperfect SIC, whereas the authors in [17] considered user fairness when obtaining the BER expressions. The authors in [18] derived an exact closed-form BER expressions under SIC error over Rayleigh fading channels in a downlink NOMA system with one base station (BS) and two users. It is worth noting that the BER performance of uplink NOMA was also widely studied. In [19], an exact average BER expression of QPSK modulation for uplink PD-NOMA with SIC was obtained under AWGN channel. In additional, the BER performance for uplink PD-NOMA in the presence of SIC error was considered in [19] and [21].

Different from [19]–[21], the authors in [22] applied joint ML detection technique instead of the SIC technique to a two-user uplink PD-NOMA system, and mathematically analyzed the BER performance. The SCMA technique has been widely studied from different aspects in, e.g., [12], [23]–[29]. In [23], [24], codeword position index based sparse code multiple access (CPI-SCMA) was proposed, which employs the idea of index modulation (IM). The CPI-SCMA can achieve better error rate performance in the high SNR region and increase the robustness under channel estimation error compare to conventional SCMA. The authors in [26], [27] developed a novel secure transmission approach over physical layer for SCMA systems in the uplink and downlink channels, respectively. In [28], the authors provided a survey on existing multidimensional constellations of SCMA for uplink Raleigh fading channels. The BER performance of those constellations were also evaluated and compared under different channel conditions. A SCMA prototype with up to 300% overloading was built in [29], with both lab testing and field experiments conducted. The testing results showed that SCMA can significantly increase (up to triple) the system throughput while still maintaining the link level performance close to orthogonal multiple access.

It is worth to mention that the current studies on PD-NOMA and SCMA are mostly carried out in a disjoint manner and little has been understood on their BER comparison. In [30], two code-domain NOMA schemes with sparse and dense codebooks, i.e., SCMA and dense code multiple access (DCMA), were analyzed and compared in terms of their link level performance and complexity. In [31], the authors compared the BERs of the following three NOMA schemes: SCMA, MUSA and PDMA. PD-NOMA and NOMA-2000 were compared with each other in terms of BER and outage probability in [32] and [33], respectively. The only existing comparison between PD-NOMA and SCMA is [34], where the authors solve the resource allocation problem of SCMA and PD-NOMA by applying the successive convex approximation method.

B. MOTIVATION AND CONTRIBUTION

As can be noted from the literature, despite a large body of literature on PD-NOMA and SCMA, a fair comparison of these two in terms of their error rate performance is still missing. Although the authors in [34] compared PD-NOMA and SCMA from the resource allocation and receiver complexity aspects, their results provide little insight on the error rate performance. Moreover, BER is a key performance indicator for the evaluation of a technique in communication systems. These motivate us to study the BER performance and make a fair comparison between the two NOMA schemes in uplink Rayleigh channels.

We briefly summarize the contributions as follows:

1) We conduct the fair comparison between two distinct NOMA techniques, namely PD-NOMA and SCMA. The BER performance of two schemes are studied and compared in uplink Rayleigh channels under the condition of the same system overloading and diversity. In particular, SCMA system with "5×10" setting (i.e., ten users communicate over five subcarriers, each active over two subcarriers) are compared with typical "1×2" and "2×4" PD-NOMA systems.
2) To attain the best error rate performance of PD-NOMA, we first view the "2×4" PD-NOMA system as a rank-deficient MIMO system and then carry out non-linear MUD by using generalized sphere decoder (GSD), which has the capability of achieving BER approaching to that of the maximum-likelihood (ML) receiver with relatively low complexity. Then, dynamic power allocation is considered for SIC and GSD aided

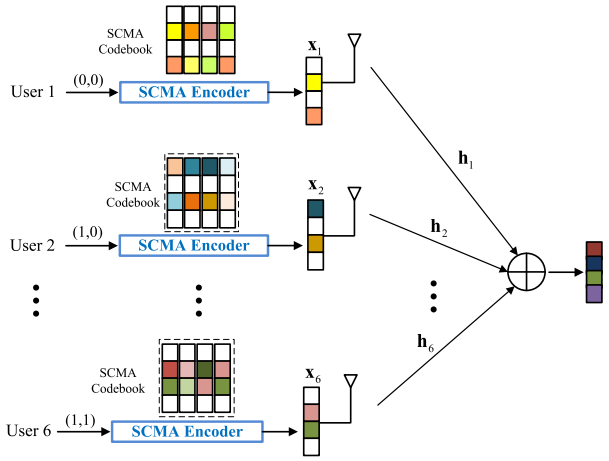

FIGURE 1. Illustration of the encoding of a 4 × 6 SCMA system where every user selects a sparse codeword from a specific codebook with size 4.

PD-NOMA and power allocation is also optimized with the aid of pairwise error probability (PEP) for the GSD based PD-NOMA. Moreover, a fair computational complexity comparison of the detection between the PD-NOMA and SCMA schemes is also carried out.

3) We also evaluate the coded BER performance with low-density parity-check (LDPC) code of the two systems and uncoded BER performance under channel estimation errors. In particular, The comparison results reveal that SCMA achieves better gain in both uncoded and coded BER performances, as well as in the presence of channel estimation errors compared to PD-NOMA.

This paper is organized as follows. In Section II, we present the system models of SCMA and PD-NOMA, as well as the multi-user detection (MUD) for SCMA. In Section III, we briefly introduce SIC for PD-NOMA. To make a fair comparison with SCMA, GSD with corresponding power allocation is also proposed for PD-NOMA in this section. Systems performance are evaluated in Section IV. Finally, Section V concludes this paper.

II. SYSTEM MODEL OF SCMA AND PD-NOMA

In this section, we present the uplink SCMA and PD-NOMA system, respectively. For simplicity but without loss of generality, we assume that the base station (BS) and all users are equipped with single antenna in both systems.

A. SCMA

Consider an uplink SCMA system with J users spreading over the same K orthogonal resources, e.g., K OFDM subcarriers. To meet the demand of massive connectivity in 5G, the number of users is normally larger than that of resources, i.e., $J > K$ and the overloading factor is defined as $\lambda = \frac{J}{K} > 1$. The process of bits mapping and SCMA codewords transmission are depicted in Fig. 1.

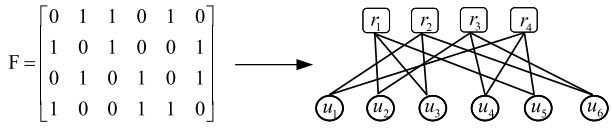

FIGURE 2. Factor graph for SCMA with $J = 6$, $K = 4$, $N = 2$, $d_r = 3$ and $d_n = 2$.

On the transmitter side, for j-th user, the SCMA encoder maps $\log_2(M)$ coded binary bits to K dimensional complex codebook set $\mathbf{X}_j$ with size M, which is defined as [35] $f_j : \mathbb{B}^{\log_2 M} \rightarrow \boldsymbol{X}_j \in \mathcal{X} \in \mathbb{C}^K, \mathbf{x}_j = f(\boldsymbol{b}_j)$, where $\boldsymbol{b}_j$ is the binary vector, M is the modulation order of the codebook. All the K-dimensional complex codewords in the SCMA codebook are sparse vectors with $N < K$ non-zero elements. It is worth noting that the sparsity inherent in the SCMA codebook can reduce the number of users occupying the same frequency resources and further allow the receiver to adopt low complexity MPA to detect signals with a near optimal MUD performance. In addition, in order to avoid any of the two users transmiting over the same N resources set, the maximum number of users is $J = \binom{K}{N} = \frac{K!}{N!(K-N)!}$. The codeword set for j-th user is given by $\mathcal{X}_j = \{\mathbf{x}_{j1}, \ldots \mathbf{x}_{jm}, \ldots, \mathbf{x}_{jM}\}$.

To further capture the sparse feature of SCMA codebooks, the indication matrix and factor graph are introduced as shown in Fig. 2. In indicator matrix $\mathbf{F}$, the set of nonzero elements in each row correspond to the users who occupy the same subcarrier while the ones in each column represent the set of subcarriers which user j utilizes to transmit signal. The element in $\mathbf{F}$ is defined as $f_{k,j}$. In the corresponding factor graph, the user node (UN) j connects with the resource node (RN) k when $f_{k,j} = 1$. In other word, each RN is connected with UNs which share the same subcarrier. We define that $\xi_k = \{j | f_{k,j} \neq 0\}$ and $\zeta_j = \{k | f_{k,j} \neq 0\}$ are the set of non-zero's position in the k-th row and j-th column, respectively. Thus, the number of users which collides over subcarrier k is d_r, i.e., $|\xi_k| = d_r$, and the number of subcarrier occupied by user j is d_u, i.e., $|\zeta_j| = d_u$.

At the receiver side, the received signal can be expressed by

$$\mathbf{y} = \sum_{j=1}^{J} \mathrm{diag}(\mathbf{h}_j)\mathbf{x}_j + \mathbf{n}, \tag{1}$$

where $\mathbf{h}_j = [h_{1,j}, h_{2,j}, \ldots, h_{K,j}]^T \in \mathbf{C}^{K\times 1}$ is the channel coefficient vector between the base station and user j, $\mathbf{x}_j = [x_{1,j}, x_{2,j}, \ldots, x_{K,j}]^T \in \mathbf{C}^{K\times 1}$ is the transmitted codeword for user j. diag$(\cdot)$ denotes the diagonalization of a matrix. $\mathbf{n} = [n_1, n_2, \ldots, n_K]^T$ is the complex Gaussian vector with the variance with zero mean and variance N_0, i.e., $\mathbf{n} \sim \mathcal{CN}(0, \sigma^2 I)$.

The above SCMA signal model can be easily extended to downlink case. In downlink channel, users' data are first supposed at the base station and then transmitted over K orthogonal subcarriers. The received signal of user j can be

expressed as

$$\mathbf{y} = \mathrm{diag}(\mathbf{h}_j) \sum_{j=1}^{J} \mathbf{x}_j + \mathbf{n}. \tag{2}$$

B. MULTI-USER DETECTION OF SCMA SYSTEM

In uplink SCMA systems, the task of BS is to decode the transmitted codewords for each user. In the following subsection, the optimal maximum-likelihood (ML) detection and MPA-based detection are introduced. We assume that the channel information is perfectly known by BS.

Given the received signal $\mathbf{y}$ and the available channel information $\mathbf{H} = (\mathbf{h}_1, \mathbf{h}_2, \ldots, \mathbf{h}_J)$, the joint optimum maximum a posteriori (MAP) detection can be utilized to estimate $\widehat{\mathbf{x}}$ by maximizing the joint a posteriori probability mass function of the transmitted codewords, which can be expressed as

$$p(\mathbf{x}|\mathbf{y}, \mathbf{H}) = p(\mathbf{x}) \cdot \exp\left(-\frac{1}{2\sigma^2} \left\| \mathbf{y} - \sum_{j=1}^{J} \mathbf{h}_j \mathbf{x}_j \right\|^2 \right). \tag{3}$$

Since each possible codeword is transmitted with equal probability by each user (i.e., $p(\mathbf{x}) = \frac{1}{M}$), the MAP detection scheme is simplified as the ML solution and can be further presented as

$$\widehat{\mathbf{x}} = \arg\min_{\mathbf{x}_j \in \chi} \left\| \mathbf{y} - \sum_{j=1}^{J} \mathbf{h}_j \mathbf{x}_j \right\|^2. \tag{4}$$

However, the execution of ML detection scheme is to exhaustively search all the possible codeword combinations for all users (i.e., the total number of possible codeword combinations is M^J, which grows exponentially with J). Thanks to the sparsity property of the SCMA codewords, the MPA detector has been applied to reduce the complexity at chip-level, specifically, from $O(M^J)$ to $O(M^{d_u})$. In MPA, the probability of users' messages are iteratively updated between the two types of nodes (RNs and UNs) associated with the underlying factor graph. Define $I_{r_k \to u_j}(\mathbf{x}_j)$ and $I_{u_j \to r_k}(\mathbf{x}_j)$ as the messages sent along edge $e_{k,j}$ from RN r_k and UN u_j, respectively. The basic procedure of original MPA detector explores the parallel scheduling strategy. At each iteration, all RNs, and subsequently all UNs pass update messages to their neighbors and change the probability of each candidate codewords. The message updates in the MPA detector can be computed as follows

$$I^t_{r_k \to u_j}(\mathbf{x}_j) = \sum_{\tilde{\mathbf{x}}_j} \left\{ \frac{1}{\sqrt{2\pi}\sigma} \exp\left(-\frac{1}{2\sigma^2} \left\| \mathbf{y}_k - \sum_{m \in \xi_k} h_{k,m} x_{k,m} \right\|^2 \right), \times \prod_{l \in \xi_k / \{j\}} I^{t-1}_{u_l \to r_k}(\mathbf{x}_l) \right\} \tag{5}$$

$$I^t_{u_j \to r_k}(\mathbf{x}_j) = \prod_{m \in \xi_j / \{k\}} I^t_{r_m \to u_j}(\mathbf{x}_j), \tag{6}$$

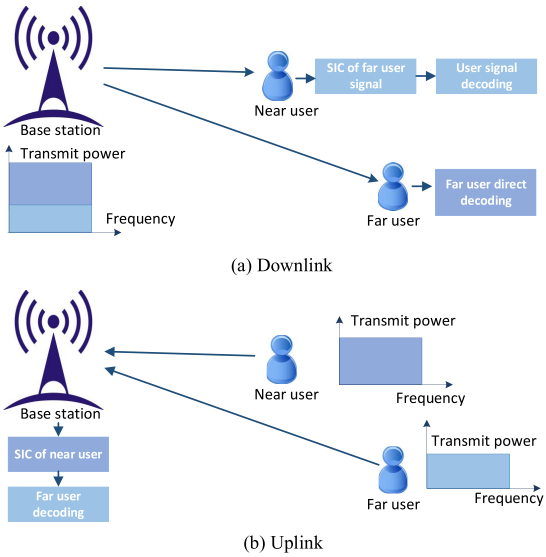

FIGURE 3. Two user NOMA scheme in downlink and uplink.

where $\sum_{\sim \mathbf{x}_j}$ denotes the summation of the codewords of user j except $\mathbf{x}_j$, t is the iteration index.

C. PD-NOMA

In PD-NOMA, multiplexing is performed in the power domain. In the downlink scenario as shown in Fig. 3, users' data are superposed at BS by allocating optimal power to each user. For the two users case, user far away from BS (far user), who experiences poor channel condition, is usually assigned with stronger power, while the user closer to BS (near user) is allocated with weaker power. In this case, the far user can detect its signal directly by treating the near user's signal as noise, while the near user first detects the far user's signal and subtracts it from the received signal before detecting its own signal. This strategy is called successive interference cancellation (SIC) [2]. However, in the uplink case, the power transmitted per user is limited by the user's maximum battery power. Power control can be used to boost up the performance of the users with better channel gain, while maintaining the performance of the users with weaker channel gains at a certain level. Let h_1 denote channel coefficient of the near user, whereas h_2 is the channel coefficient of the far user, then received signal for a single-cell uplink PD-NOMA system with two users at BS can be expressed as:

$$y = h_1 \sqrt{P\beta_1} u_1 + h_2 \sqrt{P\beta_2} u_2 + n, \tag{7}$$

where u_1 and u_2 are the transmitted signals of the near and far user, respectively. $P_i = \sqrt{P\beta_i}$ denotes the transmission power for each user. n is the additive white Gaussian noise (AWGN) with zero mean and variance σ_n^2.

In (7), users' data are transmitted on a specific subcarrier, and are not spread over multiple subcarriers, which means the diversity order (DO) in this case is 1. However, in SCMA system, as discussed in Section II, data are sparsely spread

over several subcarriers, indicating that SCMA enjoys additional DO compared to the above PD-NOMA system. For a far comparison, the DO and overloading factor are also considered to be equal, which indicates that the number of carriers occupied by each user is the same. Hence, we also consider the PD-NOMA system with $DO > 1$.

We now consider the uplink $(K \times J)$ PD-NOMA system where J users transmit signals over K subcarriers with different power levels. Let $\mathbf{h}_j = [h_{1,j}, h_{2,j}, \ldots, h_{K,j}]^T$ be the channel fading vector corresponding to user j, the elements of which are assumed to be independent and identically distributed (i.i.d) complex random variables with zero mean and unit variance, i.e., $h_{k,j} \sim \mathcal{CN}(0, 1)$. Moreover, denote $\sqrt{p_j}$ as the transmit power vector of user j and let $\mathbf{n} = [n_1, n_2, \ldots, n_K]^T$ be the AWGN vector with $n_k \in \mathcal{CN}(0, 1)$. Each user adopts quadrature phase shift keying (QPSK) modulation and the transmitted symbol is denoted as u_j. The received K dimensional signal vector has the following representation

$$\mathbf{y} = \mathbf{H}\mathbf{u} + \mathbf{n}, \tag{8}$$

where

$$\begin{aligned} \mathbf{H} &= \left[\sqrt{p_1}\mathbf{h}_1, \sqrt{p_2}\mathbf{h}_2, \ldots, \sqrt{p_J}\mathbf{h}_J\right], \\ \mathbf{u} &= [u_1, u_2, \ldots, u_J]^T. \end{aligned} \tag{9}$$

As the DO and number of users in PD-NOMA system increase, the implementation of suitable multi-user detection and interference cancellation schemes are more challenging and will incur additional computational complexity. For the downlink scenario, this may be a bottleneck because of limited processing capabilities for terminal users, as well as security concerns. However, for the uplink case, the computation is affordable at BS.

III. RECEIVER DESIGN AND POWER ALLOCATION FOR PD-NOMA

In the conventional PD-NOMA, SIC with linear complexity is adopted as the MUD. However, for SCMA systems, the MPA-based detector has higher complexity. To make a fair comparison with SCMA, we aim to conduct both SIC and ML based joint MUD for PD-NOMA. More specifically, besides SIC, generalized sphere decoder (GSD) will be introduced for PD-NOMA, which has near-ML performance while maintaining relatively low complexity. Moreover, to further evaluate and optimize the system performance PD-NOMA, we also optimize power allocation for PD-NOMA.

A. SIC

When decoding the user with strongest power at BS, signals from other users are treated as noise in the SIC process. Assuming the order of decoding is $\pi(1), \pi(2), \ldots, \pi(J)$, the input signal of j-th detection of user $\pi(j)$ is the received signal vector after subtraction of the signal component from user $\pi(j-1)$. Thus, the input signal for user $\pi(j)$ can be represented as

$$\begin{aligned} \mathbf{r}(\pi(j)) = \mathbf{h}(\pi(j))\sqrt{p(\pi(j))}u(\pi(j)) \\ + \sum_{l=j+1}^{J} \mathbf{h}(\pi(l))\sqrt{p(\pi(l))}u(\pi(l)) + \mathbf{n}. \end{aligned} \tag{10}$$

The detector could be zero forcing, minimum mean square error or ML detector for each user. When the ML is applied for j-th user, the estimated symbol vector can be written as

$$\hat{u}_{ML}(\pi(j)) = \arg\min_{u \in \mathbf{u}} \|\mathbf{r}(\pi(j)) - \mathbf{h}(\pi(j))u(\pi(j))\|. \tag{11}$$

The complexity of the ML detector depends on the total number of valid constellation combinations due to exhaustive search. For each user, the size of $\mathbf{u}$ is 2^M, where M is the modulation order. Assuming that perfect SIC is achieved at BS, the signal-to-interference and noise power ratio (SINR) of user $\pi(j)$ at SIC can be expressed as

$$SINR(\pi(j)) = \frac{p(\pi(j))\|\mathbf{h}(\pi(j))\|^2}{\sum_{l=j+1}^{J} p(\pi(l))\|\mathbf{h}(\pi(l))\|^2 + \sigma_n^2}. \tag{12}$$

B. GENERALIZED SPHERE DECODER

We consider the optimal detection based on the linear MIMO signal model in (8) by using a sphere decoder (SD). However, the system overloading is larger than 1, i.e., $J > K$, which means for random channel fading coefficients, the rank of $\mathbf{H}$ is K which is less than J. In this case, $\mathbf{H}^H\mathbf{H}$ is positive semidefinite and its Cholesky factor is not full rank [36]. Hence, conducting the optimal detection directly based on Eq. (8) by using a standard MMSE or SD detector might not work efficiently due to the rank-deficient problem. In this paper, we implement GSD proposed by Cui and Tellambura in [36] to address this issue.

Since all the elements in $\mathbf{u}$ are of constant modulus with QPSK modulation in (8), the product $\mathbf{u}^H\mathbf{u}$ is equal to J. The idea of GSD is to solve the original SD constraint by adding a constant λJ to both sides, resulting in $\|\mathbf{y} - \mathbf{H}\mathbf{u}\|^2 + \lambda J < r$, where $r = \sqrt{1 + r_{SD}^2}$ is the new hypersphere of radius in GSD. Consider the Cholesky decomposition of the positive definite matrix $\mathbf{Q} \triangleq \mathbf{H}^H\mathbf{H} + \lambda\mathbf{I}$. Consequently, $\mathbf{Q}$ can be Cholesky factorized as $\mathbf{Q} = \mathbf{D}^H\mathbf{D}$, where $\mathbf{D}$ is an upper triangular matrix. Obviously, $\mathbf{D}$ is a full-rank matrix. Moreover, let $\mathbf{r} \triangleq (\mathbf{H}\mathbf{D}^{-1})^H\mathbf{y}$ and we have

$$\begin{aligned} \hat{\mathbf{u}} &= \arg\min_{\mathbf{u} \in \mathcal{Q}^J} \left(\|\mathbf{y} - \mathbf{H}\mathbf{u}\|^2 + \lambda\mathbf{u}^H\mathbf{u}\right) \\ &= \arg\min_{\mathbf{u} \in \mathcal{Q}^J} \left(\mathbf{y}^H\mathbf{y} - \mathbf{y}^H\mathbf{H}\mathbf{u} - \mathbf{u}^H\mathbf{H}^H\mathbf{y} + \mathbf{u}^H\mathbf{Q}\mathbf{u}\right) \\ &= \arg\min_{\mathbf{u} \in \mathcal{Q}^J} \|\mathbf{r} - \mathbf{D}\mathbf{u}\|^2. \end{aligned} \tag{13}$$

The above derivation shows that the rank-deficient equation in the original ML criteria can be transformed to (13), where a standard SD can be further applied to solve the equation.

C. POWER ALLOCATION

Based on the assumption of perfect CSI acquisition, users assign appropriate power to subcarriers for optimize the system performance. Now we consider the power allocation for GSD-PD-NOMA system. Let $\mathbf{u} = [u_1, u_2, \ldots, u_J]^T$ be the transmitted signal of J users. The received signal vector in (8) can be formed in a row vector representation as

$$\mathbf{y} = \mathbf{h}_p^{\dagger}\mathbf{U} + \mathbf{n}, \tag{14}$$

where

$$\mathbf{h}_p^{\dagger} = \left[\sqrt{p_1}\mathbf{h}_1^T, \sqrt{p_2}\mathbf{h}_2^T, \ldots, \sqrt{p_J}\mathbf{h}_J^T\right]_{1\times KJ}, \tag{15}$$

and the transmitted symbol matrix is given by

$$\mathbf{U} = \begin{bmatrix} \mathbf{u} & & \mathbf{0} \\ & \ddots & \\ \mathbf{0} & & \mathbf{u} \end{bmatrix}_{KJ\times K}. \tag{16}$$

Denote M_j as the constellation size for the j-th user. We define $\{\mathbf{U}\}$ as the set of all $\prod_{j=1}^{J} M_j$ possible combined symbols of (16) and let $\mathbf{U}_a, \mathbf{U}_b \in \{\mathbf{U}\}$ be the two different elements of $\{\mathbf{U}\}$. Denote $\mathbf{u}_a^j$ and $\mathbf{u}_b^j$ as the transmitted symbols of the j-th user corresponding to $\mathbf{U}_a$ and $\mathbf{U}_b$, respectively. For the ML based detection criterion at the receiver, the conditional pair-wise error probability (PEP) can be expressed as [37]

$$P\left\{\mathbf{U}_a \to \mathbf{U}_b|\mathbf{h}_p^{\dagger}\right\} = Q\left(\sqrt{\frac{\left\|\mathbf{h}_p^{\dagger}(\mathbf{U}_a - \mathbf{U}_b)\right\|^2}{2\delta_n^2}}\right), \tag{17}$$

where $Q(x) = \frac{1}{2\pi}\int_x^{\infty} e^{-t^2/2}dt$ is the Gaussian Q-function. For the given modulation and channel matrix coefficient $\mathbf{H}$ at each data transmission, the bit error at the receiver side depends on the power allocation vector of users and the noise level. Following the approach in [37], [38], the average symbol error probability (ASEP) of the of j-th user with joint ML detection is upper bounded by

$$\begin{aligned} P_j(e) &\le \frac{1}{\prod_{j=1}^{J} M_j}\sum_{\mathbf{U}_a}\left(\sum_{\mathbf{U}_b, \mathbf{u}_a^j \ne \mathbf{u}_b^j} P\left\{\mathbf{U}_a \to \mathbf{U}_b|\mathbf{h}_p^{\dagger}\right\}\right) \\ &= \frac{1}{\prod_{j=1}^{J} M_j}\sum_{\mathbf{U}_a}\sum_{\substack{\mathbf{U}_b, \mathbf{u}_a^j \ne \mathbf{u}_b^j \\ \left[\mathbf{u}_a^1, \ldots, \mathbf{u}_a^{j-1}, \mathbf{u}_a^{j+1}, \ldots, \mathbf{u}_a^J\right] \\ = \left[\mathbf{u}_b^1, \ldots, \mathbf{u}_b^{j-1}, \mathbf{u}_b^{j+1}, \ldots, \mathbf{u}_b^J\right]}} P\left\{\mathbf{U}_a \to \mathbf{U}_b|\mathbf{h}_p^{\dagger}\right\} \\ &\quad + \frac{1}{\prod_{j=1}^{J} M_j}\sum_{\mathbf{U}_a}\sum_{\substack{\mathbf{U}_b, \mathbf{u}_a^j \ne \mathbf{u}_b^j \\ \left[\mathbf{u}_a^1, \ldots, \mathbf{u}_a^{j-1}, \mathbf{u}_a^{j+1}, \ldots, \mathbf{u}_a^J\right] \\ \ne \left[\mathbf{u}_b^1, \ldots, \mathbf{u}_b^{j-1}, \mathbf{u}_b^{j+1}, \ldots, \mathbf{u}_b^J\right]}} \\ &\quad \times P\left\{\mathbf{U}_a \to \mathbf{U}_b|\mathbf{h}_p^{\dagger}\right\}. \end{aligned} \tag{18}$$

The ASEP of system can be obtained by averaging over all single user ASEP, i.e., $P(e) = \frac{1}{J}\sum_{j=1}^{J} P_j(e)$. On the right-hand side of (18), the first part of the second term is the union bound probability of the single user case, where users' signals are detected correctly except for user j. Obviously, the optimal power allocation is to minimize $P(e)$ by considering all the combinations of $\mathbf{U}_a, \mathbf{U}_b \in \{\mathbf{U}\}$ that contribute to ASEP under the given channel condition. Since it is quite challenging (if not impossible) to deal with the optimal power allocation with the expression in (18), we only consider a suboptimal dynamic power allocation based on the single user case.

Define $\delta_{\min} = [0, \ldots, \delta_{j,\min}, \ldots, 0]^T$ as the minimum symbol-wise distance of transmitted messages, where $\delta_{j,\min}$ is the minimum symbol-wise distance for a single user. The corresponding minimum symbol-wise distance for the row vector representation in (14) is denoted as

$$\Delta_{\min} = \begin{bmatrix} \delta_{\min} & & \mathbf{0} \\ & \ddots & \\ \mathbf{0} & & \delta_{\min} \end{bmatrix}. \tag{19}$$

When channel coefficients are perfectly known at transmitter, the PEP in (18) is upper bounded by

$$\begin{aligned} P_t\left\{\mathbf{U}_a \to \mathbf{U}_b|\mathbf{h}_p^{\dagger}\right\} &\le Q\left(\sqrt{\frac{\left\|\mathbf{h}_p^{\dagger}\Delta_{\min}\right\|^2}{2\sigma_n^2}}\right) \\ &= Q\left(\sqrt{\frac{\frac{1}{K}\sum_{k=1}^{K}\left|h_{k,j}\right|^2 p_j \delta_{j,\min}^2}{2\sigma_n^2}}\right). \end{aligned} \tag{20}$$

For QPSK modulation set $\left\{a + bj | a, b \in \left\{\frac{\sqrt{2}}{2}, -\frac{\sqrt{2}}{2}\right\}\right\}$, we have $\delta_j \in \{\sqrt{2}, 2\}$, i.e., $\delta_{j_{\min}}^2 = 2$. Instead of directly minimizing the ASEP in (18), we minimize the right term in (20) to obtain a suboptimal solution. Then, the power allocation optimization can be formulated as

$$\begin{aligned} \mathbf{p} = \max \min p_j \ & \sum_{k=1}^{K}\left|h_{k,j}\right|^2, j = 1, 2, \ldots, J \\ s.t. \ & \sum_{j=1}^{J} p_j = P \end{aligned} \tag{21}$$

Let $\lambda_j = \sum_{k=1}^{K} h_{k,j}^2$, which is a known constant for user j. The above can be transformed into a standard linear programming (LP) problem. Assume the channel gain is ordered such that $\lambda_1 \le \lambda_2 \le, \ldots, \le \lambda_J$, the optimization problem can be rewritten as

$$\begin{aligned} \mathbf{p} = \arg\max \ & p_1\lambda_1 \\ s.t. \ & p_1\lambda_1 - p_m\lambda_m \le 0, m = 2, 3, \ldots, J \\ & \sum_{j=1}^{J} p_j = P \end{aligned} \tag{22}$$

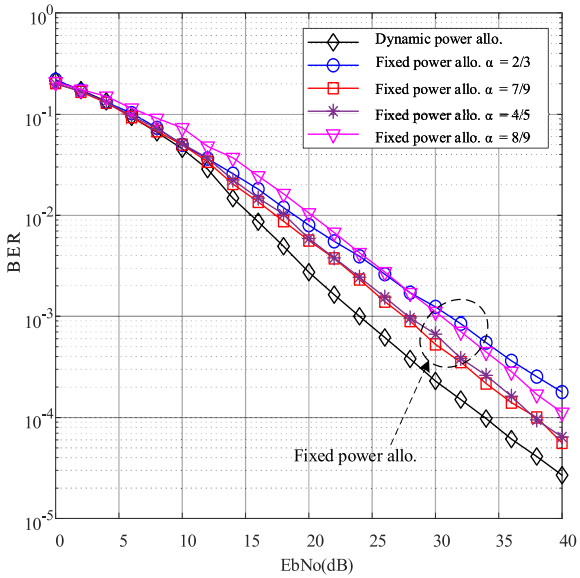

FIGURE 4. BER performance of (1 × 2)-PD-NOMA of different power imbalance with SIC receiver in uplink Rayleigh fading channels.

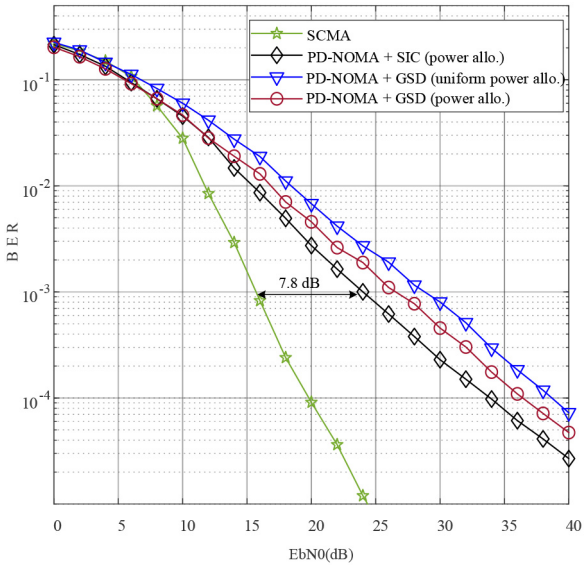

FIGURE 5. BER performance of (1 × 2)-PD-NOMA and (5 × 10)-SCMA with λ = 2 in uplink Rayleigh fading channel.

Existing approaches such as Lagrangian duality and simplex algorithm [39], [40] can be applied to solve the LP optimization problem. In fact, the objective function in (22) achieves its maximum value when the power vector satisfies

$$\frac{p_i}{p_j} = \frac{\lambda_j}{\lambda_i}, i, j = 1, 2, \ldots, J$$
$$\sum_{j=1}^{J} p_j = P. \tag{23}$$

The power vector can be easily obtained by solving the above linear equations.

IV. COMPARISONS OF SCMA AND PD-NOMA

In this section, we present the simulation results in terms of BER performance and channel estimation error for uplink PD-NOMA and SCMA over Rayleigh fading channels. We consider two PD-NOMA settings:1) $K = 1$, $J = 2$ and 2) $K = 2$, $J = 4$. In addition, $K = 5$ and $J = 10$ is considered in the SCMA system and the indicator matrix below is utilized to construct the system.

$$F = \begin{bmatrix} 1 & 1 & 1 & 1 & 0 & 0 & 0 & 0 & 0 & 0 \\ 1 & 0 & 0 & 0 & 1 & 1 & 1 & 0 & 0 & 0 \\ 0 & 1 & 0 & 0 & 1 & 0 & 0 & 1 & 1 & 0 \\ 0 & 0 & 1 & 0 & 0 & 1 & 0 & 1 & 0 & 1 \\ 0 & 0 & 0 & 1 & 0 & 0 & 1 & 0 & 1 & 1 \end{bmatrix} \tag{24}$$

A. COMPARISON OF UNCODED BER

We first evaluate the performance of (1×2) PD-NOMA with the SIC receiver, as shown in Fig. 4. For the uplink PD-NOMA with the SIC decoder, we employ both fixed power allocation and dynamic power allocation strategies according to channel gain. The fixed power allocation is carried out for different power splitting factors, i.e., $\alpha = 2/3, 7/9, 4/5, 8/9$, which have been used in [31], [32]. The user with better channel gain will be allocated with power αP, whereas the another user will transmit with power $(1-\alpha)P$. In this case, the corresponding SINRs for two users can be expressed as

$$SINR_1 = \frac{\alpha P|h_1|^2}{(1-\alpha)P|h_2|^2 + \delta_n^2},$$
$$SINR_2 = \frac{(1-\alpha)P|h_2|^2}{\delta_n^2}. \tag{25}$$

Obviously, with the fixed power allocation, the $SINR_1$ for the first user increases as α increases. From Fig. 4, for $\alpha = 2/3$, where the power imbalance is 3 dB between two users, it leads to inherent BER degradation in the high SNR region. This is because with small α (e.g., $\alpha = 2/3$), which means small $SINR_1$, the error propagation from the first detected symbol will deteriorate the performance. Although we have tried some other power splitting factor selections, no major BER performance improvement has been observed. The main observation to emphasize here is that fixed power imbalance between two users causes BER deterioration either in the low SNR or high SNR region. Therefore, we consider dynamic power allocation between users, where the power allocation satisfies $SINR_1 - SINR_2 = 5$ dB. The gap between $SINR_1$ and $SINR_2$ can help to mitigate the error propagation problem in the SIC process. As observed from Fig. 4, the PD-NOMA with dynamic power allocation exhibits 4 dB gain at BER $= 10^{-3}$ compared to the fixed power imbalance strategy.

Next, we provide the BER comparison results of the two system with same system overloading $\lambda = 2$. Fig. 5 presents the performance for (1×2)-PD-NOMA and (5×10)-SCMA system. We utilize both SIC and GSD decoders for PD-NOMA, whereas MPA is adopted in SCMA. As can be

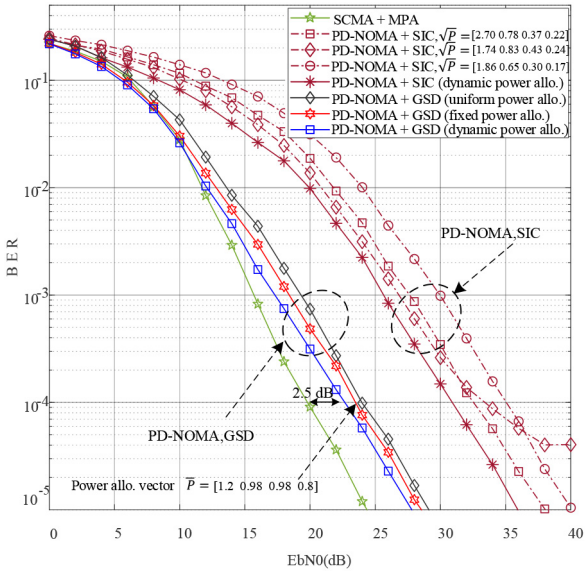

FIGURE 6. BER performance of (2 × 4)-PD-NOMA and (5 × 10)-SCMA in uplink Rayleigh fading channel. The two system have same overloading, and each user occupies same number of subcarriers.

seen from Fig. 5, the GSD detector with power imbalance between two users achieves about 2 dB gain compared to the uniform power allocation. The SIC outperforms GSD. The main reason is that for the (1×2)-PD-NOMA, the SIC with the dynamic power allocation strategy makes better utilization of the channel coefficients to optimize the system performance than that of the GSD, which is a suboptimal strategy.

For the two systems, there exists a large performance gap (10 dB) between conventional (1×2)-PD-NOMA and (5×10)-SCMA system. It is worth mentioning that the two systems have the same system overloading $\lambda = 2$, but SCMA enjoys additional diversity gain since the user-specific codewords are spread over several frequency resources. To make a more fairer comparison, we also compare the performance of two systems with the same overloading factor and number of occupied resources for each user.

Results for (2×4)-PD-NOMA and (5×10)-SCMA systems with the same overloading and diversity order are shown in Fig. 6. Similar to (1×2)-PD-NOMA system, several power allocation vectors are considered for SIC. We can observe that the BER curves of SIC lie far from the GSD curves of PD-NOMA and SCMA. The curve of PD-NOMA with $\sqrt{P} = [1.7 \;\; 0.83 \;\; 0.43 \;\; 0.24]$ has a BER floor at 4×10^{-5}. The reason is that the inappropriate power allocation between users will easy lead to error propagation, as well as the failure in decoding of users' signal with less power. In addition, when comparing SIC for (1×2) in Fig. 5 and (2×4)-PD-NOMA in Fig. 6, we see that SIC with extra diversity but the same system overloading can achieve additional BER performance gain in the high SNR region. That is to say, by introducing diversity, PD-NOMA can achieve better performance and maintain the same system overloading compared to conventional (1×2) system. However, the power allocation will be more complex as the number of users increases. For GSD, it can achieve better performance compared to the SIC aided PD-NOMA, and BER performance can be improved 2 dB with the proposed dynamic power allocation compared with uniform power allocation. In this case, the power imbalance required by PD-NOMA is maintained by different channel fading gains experienced by different users. Therefore equal power allocation would still work for the uplink systems. Finally, it is apparent that SCMA outperforms PD-NOMA by 2 dB, even when dynamic power allocation with the GSD detector is applied in PD-NOMA.

B. COMPARISON OF CODED BER

In this subsection, we compare the BER performance of two systems with LDPC codes, as shown in Fig. 7. More specifically, the (2×4)-PD-NOMA with GSD receiver and (1×2)-PD-NOMA with SIC receiver are compared with (5×10)-SCMA system. We set $\alpha = 0.8$ for the fixed power allocation of SIC receiver. The single tree-search (STS) based GSD proposed in [41] is adopted to construct the soft-output decoding of PD-NOMA system. For both SCMA and PD-NOMA, we apply two LDPC codes with rate of 0.4545 and 0.5882. The information bits are fixed with 200 bits. For example, when the second rate 0.5882 is used, the LDPC block consists of 200 bits and 340 bits before and after encoding, respectively. From Fig. 7, we have the following key observations:

1) For the two LDPC rates, the GSD with power allocation achieves 3dB gain and SIC receiver with dynamic power allocation achieve about 2 dB gain over the fixed power allocation for the BER between 10^{-5} and 10^{-3}. 2) The coding gain between SCMA system and PD-NOMA system with conventional SIC receiver is same for the two rates, where 3dB gain is attained by SCMA for the BER between 10^{-5} and 10^{-2}. 3) It is interesting to see GSD detector with dynamic power allocation works well at rate of 0.4545 and achieves almost 8.5dB coding gain compared to that of 0.5882. When considering the power allocation for PD-NOMA system, GSD can achieve better uncoded BER performance than SCMA, which is shown in Fig. 6. In this case, the performance gap becomes marginal between SCMA and GSD based PD-NOMA when LDPC rate is small in Fig. 7b.

C. COMPARISON OF UNCODED BER WITH CHANNEL ESTIMATION ERROR

In the previous section, we assume perfect SIC and channel estimation. In practical wireless systems, however, it is quite challenging to obtain perfect channel coefficients. The channel estimation error (CEE) will affect the decoding performance. Hence, it is of practical interest to compare the BER performance of PD-NOMA and SCMA in the presence of channel estimation errors. Considering CEE, we

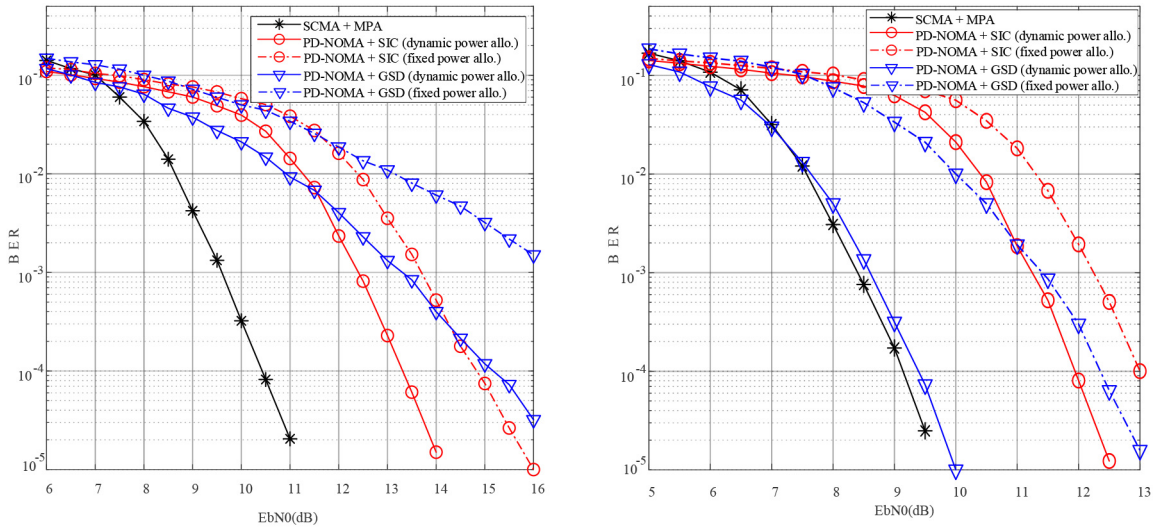

(a) LDPC rate = 0.5822 (b) LDPC rate = 0.4545

FIGURE 7. Coded BER performance of PD-NOMA and SCMA in uplink Rayleigh fading channel.

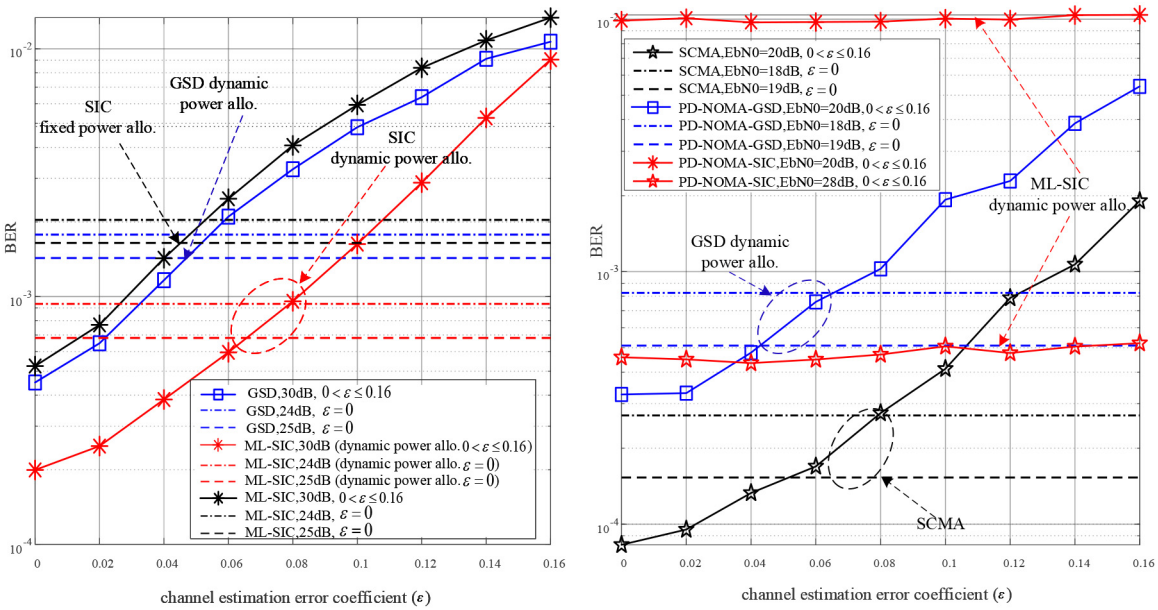

(a) (1×2) PD-NOMA systems (b) (2×4) PD-NOMA and (5×10) SCMA systems

FIGURE 8. Uncoded BER comparison with CEE coefficients ε in uplink Raleigh channels for EbN0 at 30dB and 20dB respectively.

will model the estimated channel coefficients for user j as follows [30]

$$\hat{\mathbf{h}}_j = \mathbf{h}_j \cdot \left(1 + \varepsilon \cdot \Delta_j\right), \tag{26}$$

where $\hat{\mathbf{h}}_j$ is the estimate of the original channel $\mathbf{h}_j$. $0 < \varepsilon \leq 1$ is the normalized CEE factor and Δ_j is the uniform distributed and complexed-value random variable over the unitary circle $|x| \leq 1$.

In Fig. 8, we compare the uncoded BER performance of SCMA, GSD and SIC PD-NOMA with channel estimation error $\varepsilon \in [0, 0.16]$. Fig. 8(a) depicts the two-users uplink scenario with EbN0 = 30 dB. The BER performances at EbN0 = 30 dB with CEE are denoted by "BER (GSD, 30 dB, $0 < \varepsilon \leq 0.16$), BER (SIC, 30 dB, $0 < \varepsilon \leq 0.16$)" and "BER (SIC, 30 dB, dynamic power allo. $0 < \varepsilon \leq 0.16$)", respectively. It is apparent that when $0 < \varepsilon$, the CEE leads to BER performance deterioration, which has a similar effect to that of a decreased EbN0.

To examine which detector is more resilient to CEE, we have also simulated BER at EbN0 = 24 dB and EbN0 = 25 dB as shown by the dash line. Let us define $\varepsilon_i^{(j)}$, $\{i = 1, 2, 3; j = 1, 2\}$, where superscript (j) denotes the two SNR values and the subscript i indicates three different decoding schemes, i.e., GSD, SIC with fixed power allocation and SIC

with dynamic power allocation, respectively. For example, $\varepsilon_1^{(1)}$ and $\varepsilon_1^{(2)}$ are the CEEs of GSD, which satisfy

$$\begin{aligned} &BER\Big(GSD, EbN0 = 30dB, \varepsilon_1^{(1)}\Big) \\ &\quad = BER(GSD, EbN0 = 24dB, \varepsilon = 0), \\ &BER\Big(GSD, EbN0 = 30dB, \varepsilon_1^{(2)}\Big) \\ &\quad = BER(GSD, EbN0 = 25dB, \varepsilon = 0). \end{aligned} \tag{27}$$

Similarly, we can obtain $\varepsilon_2^{(1)}$, $\varepsilon_2^{(2)}$ for SIC, and $\varepsilon_3^{(1)}$, $\varepsilon_2^{(2)}$ for SIC (dynamic power allo.) at EbN0 = 24 dB and EbN0 = 25 dB, respectively. For BERs of the (1×2)-PD-NOMA system shown in Fig. 8(a), we have $\varepsilon_1^{(1)} \approx 0.063$, $\varepsilon_2^{(1)} \approx 0.044$ and $\varepsilon_3^{(1)} \approx 0.09$, indicating that the GSD based PD-NOMA is more sensitive to CEE while the SIC with dynamic power allocation is most robust among the others. Alternatively, when comparing $\varepsilon_1^{(2)} \approx 0.078$, $\varepsilon_2^{(2)} = 0.052$ and $\varepsilon_3^{(2)} \approx 0.12$, the assertion is the same.

For the BERs of (2×4)-PD-NOMA and (5×10)-SCMA systems shown in Fig. 8(b), we also consider $\varepsilon_i^{(j)}$ with superscript (j), $\{j = 1, 2\}$ denoting the two SNR values (18 dB and 19 dB) and the subscript i, $\{i = 1, 2, 3\}$ for SCMA, GSD and SIC aided PD-NOMA, respectively. It is clear that the GSD based PD-NOMA is more resilient than SCMA as $\varepsilon_1^{(1)} \approx 0.05$, $\varepsilon_2^{(1)} \approx 0.04$. As for the PD-NOMA with SIC, the BER changes slowly with CEE at SNR = 20 dB. The reason is that the BER performance is mainly dominated by limited SINR with the increasing number of users. Here, we also simulated the CEE for SIC at SNR = 28 dB (BER $\approx 5 \times 10^{-4}$), which provides the same result.

D. COMPARISON OF COMPLEXITY

In this subsection, we compare the complexities of the GSD and SIC detectors for PD-NOMA and MPA detector for SCMA system, respectively. As for the SCMA system, the MPA in log-domain is adopted in the simulation results, which has a modest computational complexity. The addition and multiplication operations in Log-MPA are $(Jd_uM^{d_r}N_{iter} + KM^{d_r} - N_{iter}MJd_u)$ and $(Jd_uM^{d_r}(N_{iter}d_r + 1) + JM(N_{iter}d_u + 1)(d_u - 1))$ respectively, where N_{iter} refers to the number of MPA iterations [42]. For the GSD detector, the complexity is proportional to the number of nodes visited on the tree and consequently, to the number of points visited in the spheres of radius and constellation size. More specifically, for a wide range of SNRs and numbers of antennas, the expected complexity is polynomial, in fact, often roughly cubic [43]. In PD-NOMA system, the SIC detector has the linear complexity, which is much lower than that of GSD and MPA. The floating point (FLOP) operations which refers to either a complex multiplication or a complex addition is calculated to further compare the computation complexity of the three detectors. We define the normalized complexity as follows:

$$\text{Normalized Complexity} \triangleq \frac{\text{Number of FLOPs}}{J \log_2 M}. \tag{28}$$

TABLE 1. Complexity comparison for PD-NOMA and SCMA systems ($M = 4$).

Receiver types	Normalized complexity
(5×10)-SCMA+ MPA	9502
(1×2)-PD-NOMA + GSD	103
(2×4)-PD-NOMA + GSD	675
(1×2)-PD-NOMA + SIC	15.5
(2×4)-PD-NOMA+ SIC	21.5

In (5×10)-SCMA system, for decoding convergence, we set $N_{iter} = 10$ in the simulation, and the complexity of the GSD detector is averaged over the SNR range [0, 30]dB with step size 2dB. As can be seen in Table 1, the complexity of SCMA receiver is much higher than that of PD-NOMA receiver.

V. CONCLUSION

In this paper, we have carried out the bit error rate comparison for two distinct overloaded NOMA systems, i.e., PD-NOMA and SCMA. For PD-NOMA, in addition to SIC, we also applied the GSD detector with proposed dynamic power imbalance between users to optimize the system performance. We provided comprehensive simulation results for both SCMA and PD-NOMA. For PD-NOMA with SIC receiver, our results demonstrated that dynamic power allocation outperforms fixed power allocation in the uplink link Rayleigh fading channel. Moreover, by increasing the diversity (e.g., 2×4 PD-NOMA system), while maintaining the same overloading for PD-NOMA, we can enhance the BER performance. The third important observation is that although fairness between two systems and BER optimization for PD-NOMA have been explicitly taken into consideration, SCMA still outperforms PD-NOMA in terms of uncoded and coded BER, as well as in the presence of channel estimation errors.

VI. ACKNOWLEDGMENT

The authors also would like to acknowledge the support of the University of Surrey 5GIC (http://www.surrey.ac.uk/5gic) members for this work.

REFERENCES

[1] C. Bockelmann *et al.*, "Massive machine-type communications in 5G: Physical and MAC-Layer solutions" *IEEE Commun. Mag.*, vol. 54, no. 9, pp. 59–65, Sep. 2016.

[2] L. Dai, B. Wang, Y. Yuan, S. Han, I. Chih-lin, and Z. Wang, "Non-orthogonal multiple access for 5G: Solutions, challenges, opportunities, and future research trends," *IEEE Commun. Mag.*, vol. 53, no. 9, pp. 74–81, Sep. 2015.

[3] Z. Ding, X. Lei, G. K. Karagiannidis, R. Schober, J. Yuan, and V. K. Bhargava, "A survey on non-orthogonal multiple access for 5G networks: Research challenges and future trends," *IEEE J. Sel. Areas Commun.*, vol. 35, no. 10, pp. 2181–2195, Oct. 2017.

[4] Z. Wei, J. Yuan, D. W. K. Ng, M. Elkashlan, and Z. Ding, "A survey of downlink non-orthogonal multiple access for 5G wireless communication networks," *ZTE Commun.*, vol. 14, no. 4, pp. 17–26, Oct. 2016.

[5] L. Dai, B. Wang, Z. Ding, Z. Wang, S. Chen, and L. Hanzo, "A survey of non-orthogonal multiple access for 5G," *IEEE Commun. Surveys Tuts.*, vol. 20, no. 3, pp. 2294–2323, 3rd Quart., 2018.

[6] Y. Saito, Y. Kishiyama, A. Benjebbour, T. Nakamura, A. Li, K. Higuchi, "Non-orthogonal multiple access (NOMA) for cellular future radio access," in *Proc. IEEE Veh. Technol. Conf. (IEEE VTC Spring)*, Jun. 2013, pp. 1–5.

[7] S. M. R. Islam, N. Avazov, O. A. Dobre, and K.-S. Kwak, "Power-domain non-orthogonal multiple access (NOMA) in 5G systems: Potentials and challenges," *IEEE Commun. Surveys Tuts.*, vol. 19, no. 2, pp. 721–742, 2nd Quart., 2017.

[8] Z. Ding, F. Adachi, and H. V. Poor, "The application of MIMO to non-orthogonal multiple access," *IEEE Trans. Wireless Commun.*, vol. 15, no. 1, pp. 537–552, Jan. 2016.

[9] Z. Ding, L. Dai, and H. V. Poor, "MIMO-NOMA design for small packet transmission in the Internet of Things," *IEEE Access*, vol. 4, pp. 1393–1405, 2016.

[10] Y. Liu, Z. Ding, M. Elkashlan, and H. V. Poor, "Cooperative non-orthogonal multiple access with simultaneous wireless information and power transfer," *IEEE J. Sel. Areas Commun.*, vol. 34, no. 4, pp. 938–953, Apr. 2016.

[11] R. Hoshyar, F. P. Wathan, and R. Tafazolli, "Novel low-density signature for synchronous CDMA systems over AWGN channel," *IEEE Trans. Signal Process.*, vol. 56, no. 4, pp. 1616–1626, Apr. 2008.

[12] M. Al-Imari, M. A. Imran, R. Tafazolli, and D. Chen, "Performance evaluation of low density spreading multiple access," in *Proc. IEEE Int. Wireless Commun. Mobile Comput. Conf. (IWCMC)*, Limassol, Cyprus, Aug. 2012, pp. 383–388.

[13] M. Al-Imari, P. Xiao, M. A. Imran, and R. Tafazolli, "Uplink non-orthogonal multiple access for 5G wireless networks," in *Proc. IEEE 11th Int. Symp. Wireless Commun. Syst. (ISWCS)*, Barcelona, Spain, Aug. 2014, pp. 781–785.

[14] H. Nikopour and H. Baligh, "Sparse code multiple access," in *Proc. IEEE PIMRC*, London, U.K., Sep. 2013, pp. 332–336.

[15] M. Taherzadeh, H. Nikopour, A. Bayesteh, and H. Baligh, "SCMA codebook design," in *Proc. IEEE VTC-Fall*, Las Vegas, NV, USA, Sep. 2014, pp. 1–5.

[16] L. Bariah, S. Muhaidat, and A. Al-Dweik, "Error probability analysis of non-orthogonal multiple access over Nakagami-*m* fading channels," *IEEE Trans. Commun.*, vol. 67, no. 2, pp. 1586–1599, Feb. 2019.

[17] T. Assaf, A. Dweik, M. Moursi, and H. Zeineldin, "Exact BER performance analysis for downlink NOMA systems over Nakagami-*m* fading channels," *IEEE Access*, vol. 7, pp. 134539–134555, Sep. 2019.

[18] I. H. Lee and J. B. Kim, "Average symbol error rate analysis for non-orthogonal multiple access with M-ary QAM signals in Rayleigh fading channels," *IEEE Commun. Lett.*, vol. 23, no. 8, pp. 1328–1331, Aug. 2019.

[19] X. Wang, F. Labeau, and L. Mei, "Closed-form BER expressions of QPSK constellation for uplink non-orthogonal multiple access," *IEEE Commun. Lett.*, vol. 21, no. 10, pp. 2242–2245, Oct. 2017.

[20] F. Kara and H. Kaya, "BER performances of downlink and uplink NOMA in the presence of SIC errors over fading channels," *IET Commun.*, vol. 12, no. 15, pp. 1834–1844, Sep. 2018.

[21] H. Haci, H. Zhu, and J. Wang, "Performance of non-orthogonal multiple access with a novel asynchronous interference cancellation technique," *IEEE Trans. Commun.*, vol. 65, no. 3, pp. 1319–1335, Mar. 2017.

[22] J. S. Yeom, H. S. Jang, K. S. Ko, and B. C. Jung, "BER performance of uplink NOMA with joint maximum-likelihood detector," *IEEE Trans. Veh. Technol.*, vol. 68, no. 10, pp. 10295–10300, Oct. 2019.

[23] K. Lai, J. Lei, L. Wen, and G. Chen, "Codeword position index modulation design for sparse code multiple access system," *IEEE Trans. Veh. Technol.*, vol. 69, no. 11,, pp. 13273–13288, Nov. 2020.

[24] K. Lai, L. Wen, J. Lei, G. Chen, P. Xiao, and A. Maaref, "Codeword position index based sparse code multiple access system," *IEEE Wireless Commun. Lett.*, vol. 8, no. 3, pp. 737–740, Jun. 2019.

[25] A. Bayesteh, H. Nikopour, M. Taherzadeh, H. Baligh, and J. Ma, "Low complexity techniques for SCMA detection," in *Proc. IEEE Glob. Commun. Conf. Workshops (IEEE Globecom Workshops)*, San Diego, CA, USA, Dec. 2015, pp. 1–6.

[26] K. Lai, L. Wen, J. Lei, G. Chen, P. Xiao, and A. Maaref, "Secure transmission with interleaver for uplink sparse code multiple access system," *IEEE Wireless Commun. Lett.*, vol. 8, no. 2, pp. 336–339, Apr. 2019.

[27] K. Lai, J. Lei, L. Wen, G. Chen, W. Li, and P. Xiao, "Secure transmission with randomized constellation rotation for downlink sparse code multiple access system," *IEEE Access*, vol. 6, pp. 5049–5063, 2018.

[28] M. Vameghestahbanati, I. Marsland, R. H. Gohary, and H. Yanikomeroglu. *Multidimensional Constellations for Uplink SCMA System–A Comparative Study*. 2018. [Online]. Available: arXiv:1804.05814.

[29] L. Lu, Y. Chen, W. Guo, H. Yang, Y. Wu, and S. Xing, "Prototype for 5G new air interface technology SCMA and performance evaluation," *China Commun.*, vol. 12, no. 1, pp. 38–48, Dec. 2015.

[30] Z. Liu and L. Yang, *Sparse or Dense: A Comparative Study of Code-Domain NOMA Systems*. 2020. [Online]. Available: arXiv:2009.04148.

[31] B. Wang, K. Wang, Z. Lu, T. Xie, and J. Quan, "Comparison study of non-orthogonal multiple access schemes for 5G," in *Proc. IEEE ISBMSB*, Ghent, Belgium, Jun. 2015, pp. 1–5.

[32] A. Khansa, Y. Yin, G. Gui, and H. Sari, "Power-domain NOMA or NOMA-2000?" in *Proc. IEEE APCC*, Ho Chi Minh City, Vietnam, 2019, pp. 336–341.

[33] I. Cosandal, M. Koca, E. Biglieri, and H. Sari, "NOMA-2000 versus PD-NOMA: An outage probability comparison," accepted by *IEEE Commun. Lett.*, vol. 25, no. 2, pp. 427–431, Feb. 2021.

[34] M. Moltafet, N. M. Yamchi, M. R. Javan, and P. Azmi, "Comparison study between PD-NOMA and SCMA," *IEEE Trans. Veh. Technol.*, vol. 67, no. 2, pp. 1830–1834, Feb. 2018.

[35] Z. Liu, P. Xiao, and M. Zeina, "Power-imbalanced low-density signatures (LDS) from eisenstein numbers," in *Proc. IEEE APWCS*, Singapore, Aug. 2019, pp. 1–5.

[36] T. Cui and C. Tellambura, "An efficient generalized sphere decoder for rank-deficient MIMO systems," in *Proc. IEEE VTC-Fall*, Los Angeles, CA, USA, Sep. 2004, pp. 3689–3693.

[37] J. Bao, Z. Ma, G. K. Karagiannidis, M. Xiao, and Z. Zhu, "Joint multiuser detection of multidimensional constellations over fading channel," *IEEE Trans. Commun.*, vol. 65, no. 1, pp. 161–172, Jan. 2017.

[38] X. Zhu and R. D. Murch, "Performance analysis of maximum likelihood detection in a MIMO antenna system," *IEEE Trans. Commun.*, vol. 50, no. 2, pp. 187–191, Feb. 2002.

[39] G. Kalal, "Linear programming, the simplex algorithm and simple polytopes," *Math. Program.*, vol. 79, pp. 217–233, Oct. 1997.

[40] R. J. Vanderbei, *Linear Programming: Foundations and Extensions*. Norwell, MA, USA: Kluwer, vol. 37, Jun. 2001.

[41] C. Studer and H. Bölcskei, "Soft-input soft-output single tree-search sphere decoding," *IEEE Trans. Inf. Theory*, vol. 56, no. 10, pp. 4827–4842, Oct. 2010.

[42] C. Zhang, Y. Luo, and Y. Chen, "A low-complexity SCMA detector based on discretization," *IEEE Trans. Wireless Commun.*, vol. 17, no. 4, pp. 2333–2345, Apr. 2018.

[43] B. Hassibi and H. Vikalo, "On the sphere-decoding algorithm I. Expected complexity," *IEEE Trans. Signal Process.*, vol. 53, no. 8, pp. 2806–2818, Aug. 2005.

QU LUO (Graduate Student Member, IEEE) received the bachelor's degree from the Chongqing University of Posts and Telecommunications, Chongqing, China, in 2016, and the master's degree from the University of Electronic and Science Technology of China in 2019. He is currently pursuing the Ph.D. degree with the 5G Innovation Centre, University of Surrey, U.K. His research focuses on deep learning and non-orthogonal multiple access.

PENGYU GAO received the B.S. and M.S. degrees from UESTC, Chengdu, China, in 2016 and 2019, respectively. He is currently pursuing the Ph.D. degree in the 5GIC, University of Surrey, U.K. His research focuses on compressed sensing, grant-free multiple access, and SCMA.

ZILONG LIU (Senior Member, IEEE) received the bachelor's degree from the School of Electronics and Information Engineering, Huazhong University of Science and Technology, China, in 2004, the master's degree from the Department of Electronic Engineering, Tsinghua University, China, in 2007, and the Ph.D. degree from the School of Electrical and Electronic Engineering, Nanyang Technological University (NTU), Singapore, in 2014. He is a Lecturer (Assistant Professor) with the School of Computer Science and Electronics Engineering, University of Essex. From January 2018 to November 2019, he was a Senior Research Fellow with the Institute for Communication Systems, Home of the 5GIC, University of Surrey. Prior to his career in U.K., he spent nine and half years in NTU, first as a Research Associate (July 2008 to October 2014) and then a Research Fellow (November 2014 to December 2017). His Ph.D. thesis "Perfect- and Quasi- Complementary Sequences," focusing on fundamental limits, algebraic constructions, and applications of complementary sequences in wireless communications, has settled a few long-standing open problems in the field. His research lies in the interplay of coding, signal processing, and communications, with a major objective of bridging theory and practice as much as possible. Recently, he has developed an interest in applying machine learning for wireless communications. He is a General Co-Chair of the 10th International Workshop on Signal Design and its Applications in Communications (2022) and a TPC Co-Chair of the 2020 IEEE International Conference on Advanced Networks and Telecommunications Systems. Besides, he was/is a TPC member of a number of IEEE Conferences/Workshops (e.g., ICC, WCSP, GLOBECOM, ICCS, SETA, and ISIT). He is an Associate Editor of IEEE WIRELESS COMMUNICATIONS LETTERS, IEEE ACCESS, and *Frontiers in Communications and Networks*. Details of his research can be found at: https://sites.google.com/site/zilongliu2357.

LIXIA XIAO (Member, IEEE) received the B.E., M.E., and Ph.D. degrees from the UESTC in 2010, 2013, and 2017, respectively. From 2016 to 2017, she was a visiting student with the School of Electronics and Computer Science, University of Southampton. From 2018 to 2019, she has been a Research Fellow with the Department of Electrical Electronic Engineering, University of Surrey. She is currently a Full Professor with the Wuhan National Laboratory for Optoelectronics, Huazhong University of Science and Technology. In particular, she is very interested in signal detection and performance analysis of wireless communication systems. Her research interests include wireless communications and communication theory.

ZEINA MHEICH received the Dipl.Ing. degree in telecommunications and computers from the Faculty of Engineering, Lebanese University, Beirut, Lebanon, in 2009, and the M.Sc. and Ph.D. degrees from University Paris Sud 11, Orsay, France, in 2010 and 2014, respectively. From January 2015 to February 2017, she was a Research Engineer with the CEA-LETI, Grenoble, France. She was a Postdoctoral Researcher with the IMT Atlantique, Brest, France, until August 2017. She is currently a Research Fellow with 5GIC, University of Surrey, Guildford, U.K. Her research interests are in the areas of coding, wireless communications, and information theory.

PEI XIAO (Senior Member, IEEE) is a Professor of Wireless Communications with the Institute for Communication Systems, 5GIC, University of Surrey. He is the Technical Manager with 5GIC, leading the research team in the new physical layer work area, and coordinating/supervising research activities across all the work areas within 5GIC. He was worked with Newcastle University and Queen's University Belfast. He also held positions with Nokia Networks, Finland. He has published extensively in the fields of communication theory, RF and antenna design, signal processing for wireless communications, and is an inventor on over ten recent 5GIC patents addressing bottleneck problems in 5G systems.

AMINE MAAREF (Senior Member, IEEE) received the Ph.D. degree in telecommunications from INRS, Quebec University in 2007.

Since 2011, he has been with the Huawei Technologies Canada Research Center, Ottawa, ON, Canada, where he currently holds the position of a Senior Principal Engineer, focusing on 5G/6G radio access design. He is a LTE and NR Technical Expert and has been part of Huawei Technologies 3GPP RAN1 standard delegation, during which time he was actively involved in 5G NR Release 15/16 standardization. Prior to joining Huawei, he was with Mitsubishi Electric Research Labs, Cambridge, MA, USA, as a Research Scientist, where he conducted advanced research in broadband mobile communications and was actively involved in 3GPP LTE/LTE-Advanced and WiMAX IEEE 802.16m standardization. Over the last 20 years, he has coauthored more than 100 international peer-reviewed publications and standard contributions in the relevant fora, holds more than 350 worldwide awarded patents and pending patent applications, and received numerous prestigious awards for his outstanding research and scholarly achievements. He was the Guest Editor for several special issues of IEEE journals and magazines and was the founding Managing Editor of IEEE 5G/Future Networks Tech Focus. From 2014 to 2020, he served as an Editor of the IEEE TRANSACTIONS ON WIRELESS COMMUNICATIONS and currently serves as an Editor of IEEE TRANSACTIONS ON COMMUNICATIONS.